

# Lawrence Berkeley National Laboratory

## Recent Work

### Title

Interplay between Swelling Kinetics and Nanostructure in Perfluorosulfonic Acid Thin-Films:  
Role of Hygrothermal Aging

### Permalink

<https://escholarship.org/uc/item/4r1005g0>

### Journal

ACS Applied Polymer Materials, 1(4)

### ISSN

2637-6105

### Authors

Tesfaye, M  
Kushner, DI  
Kusoglu, A

### Publication Date

2019-04-12

### DOI

10.1021/acsapm.9b00005

Peer reviewed

**On the Interplay between Swelling Kinetics and Nanostructure in PFSA Thin-films:**  
**Role of Hygrothermal Ageing**

Meron Tesfaye <sup>†, ‡</sup>, Douglas I. Kushner <sup>‡</sup>, Ahmet Kusoglu <sup>‡, \*</sup>

<sup>†</sup> Chemical and Biomolecular Engineering, University of California Berkeley, Berkeley, CA,  
94720

<sup>‡</sup> Energy Storage & Distributed Resources Division, Lawrence Berkeley National Laboratory,  
Berkeley, CA, 94720

\* Author to whom correspondence should be addressed: [akusoglu@lbl.gov](mailto:akusoglu@lbl.gov)

## 11    **Abstract**

12            Impacts of processing, storage, and operation on thin-film perfluorosulfonic-acid (PFSA)  
13 ionomer coatings used in electrodes of electrochemical devices remains unestablished. In this  
14 work, alteration of structure-function relationship in ionomers is achieved via exposure to elevated  
15 temperature and humidity (hygrothermal ageing). Findings reflect a strong inverse correlation  
16 between ageing-induced ionomer thin-film domain orientation and water-transport kinetics  
17 evaluated from swelling. Impact of ageing is shown to be more pronounced on platinum, due to  
18 interactions with PFSA, as evidenced by greater increase in nano-domain orientation parallel to  
19 substrate accompanied by reduced water transport, in contrast to silicon support.

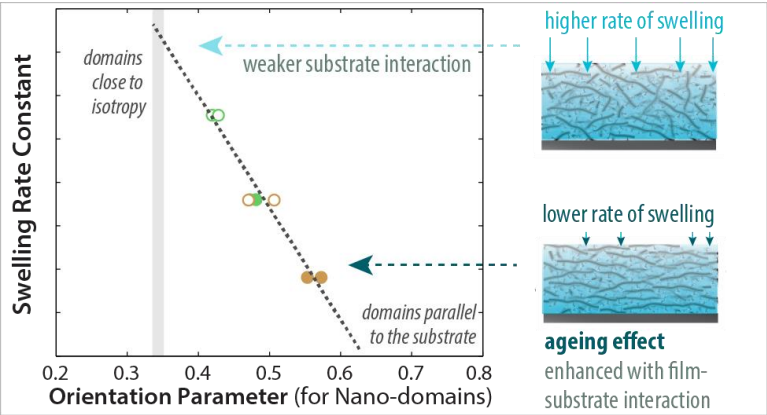
20

## 21    **Keywords:**

22 ionomer thin-films, hygrothermal ageing, nanostructure, domain orientation, time constant, water  
23 transport kinetics

24

25



Perfluorosulfonic-acid (PFSA) ionomers serve as benchmark polymer electrolytes for various clean-water and energy-conversion electrochemical technologies.<sup>1</sup> Integral to its ion- and water-transport capabilities is PFSA's phase-separated structure, which is enhanced upon hydration of its -SO<sub>3</sub>H end groups and maintained by the mechanical stability of its inert backbone matrix.<sup>1</sup> As a random copolymer lacking well-defined structure, comprehension of PFSA's intrinsic structure-function relationship has heavily dependent on processing conditions (i.e. pre-treatment, cation contamination, *etc.*), thermal history (unmanned, annealed, hot-pressed, *etc.*), and external stimuli (i.e. humidity, solvent, *etc.*).<sup>1,2</sup> However, engineering high-performance ionomers requires establishment of fundamental relationship between morphology of PFSA and properties that dictate performance.<sup>2</sup> This is even more consequential for PFSA thin-films (nanometers in thickness), as local interfaces and interactions impose additional constraints that limit critical properties, impeding electrode performance in energy-conversion devices.<sup>3,4</sup> Various examples of confinement-driven limitations in thin-film ionomers include decreased water uptake, diffusivity, ion conductivity, accompanied by an overall increase in transport resistance and mechanical stiffness.<sup>1,3-7</sup> While these property changes have been ascribed to substrate-dependent morphological changes, interfacial interactions, and finite-size driven enthalpic and entropic strains, few have resulted in definitive predictive correlations.<sup>5,8</sup> To that effect, this study aims to explicitly correlate substrate-dependent morphology (nano-structural orientation) with water-sorption kinetics (swelling property) by employing hygrothermal ageing.

While some environmental conditions intrinsic to device operation (such as hydration) are necessary to maintain PFSA functionality, they can also permanently alter

structure and functionality over time.<sup>9–11</sup> Notably, prolonged exposure of bulk PFSA to hot and humid conditions (hygrothermal ageing) results in dramatic changes in ionomer properties, altering ionomer's morphology, increasing mechanical properties and reducing water uptake and conductivity.<sup>9–13</sup> Although no such explorations on the impact of ageing in PFSA thin-films exists thus far, the technique of prolonged solvent exposure and different processing conditions are frequently employed in block-copolymer thin-films to access different morphologies.<sup>14–16</sup> In supported ionomer thin-films, similar to ionomers present in electrodes, morphological changes cannot be decoupled from supporting substrates. Recent findings have reported ionomer thin-film swelling property depends on the chemical composition of substrates (platinum/oxidized platinum (Pt/PtO<sub>x</sub>), gold (Au), and carbon (C)), which may even be dictated during film formation, highlighting the key role substrate interactions play in controlling film behavior.<sup>3,7,17</sup> Thin-films exhibit phase-separated domains under humidification, similar to a membrane, but with anisotropy driven by substrate and confinement effects.<sup>3,18</sup> While thin-films on silicon substrates with native oxide (Si/SiO<sub>x</sub>) exhibits close to isotropic patterns (random domain orientation), films on hydrophobized Si or metallic substrates exhibit anisotropic domain orientation, which is further enhanced for film thicknesses <50 nm.<sup>1,3</sup> This work demonstrates a direct link between ionomer thin-film swelling, which serves as proxy for ion conductivity and water transport, to substrate dependent nano-structural orientation as accessed by hygrothermal ageing.

In this study, 30–40nm thin-films of PFSA with long- and medium-side-chain length (Nafion and 3M respectively) were spun-cast on Si/SiO<sub>x</sub> and Pt/PtO<sub>x</sub> substrates to mimic ionomers in electrochemical electrodes. The films were then hygrothermally aged for 2–4

days in an environmental chamber held at 85% relative humidity (RH) and a temperature  
 of 70 °C. Structural changes caused by hygrothermal ageing are investigated via *in-situ*  
 grazing incidence small-angle X-ray scattering (GISAXS). Fig. 1 summarizes the GISAXS  
 patterns of unaged (as-cast) and aged PFSA thin-films on Si/SiO<sub>x</sub> and Pt/PtO<sub>x</sub> support. An  
 ionomer peak (at  $q_{\text{peak}} = 2$  to  $2.5 \text{ nm}^{-1}$ ) is apparent in all, and more pronounced in aged thin-  
 films (Fig. 1a), signifying the phase-separated nanostructure with a correlation length of  $d$   
 $= 2\pi/q_{\text{peak}} = 2.5$  to  $3 \text{ nm}$ . Upon hydration, the ionomer peak shifts to lower  $q$  (large  $d$ ) due  
 to incorporation of water molecules into hydrophilic nano-domains. Interestingly, changes  
 in peak position as well as peak shape upon hydration are less distinct for aged films where  
 the hydrophilic-domain network appears to already be expanded and set as a result of  
 ageing.<sup>3,18</sup> (See SI for further discussion). The high-intensity regions around the specular  
 peak in the GISAXS images (Fig. 1a) highlight the hygrothermal ageing-induced  
 anisotropic structure. To analyze structural anisotropy, the intensity distributions around  
 the ionomer peak position ( $q_{\text{peak}} = 2.5 \pm 0.25 \text{ nm}^{-1}$ ) are taken from the 2D GISAXS spectra  
 and plotted as a function of azimuthal angle,  $I(\chi)$  (Fig. 1b). Films on the Si/SiO<sub>x</sub> substrate  
 exhibit a low degree of anisotropy and closely follow the ideal isotropic distribution ( $I(\chi)$   
 $= \text{constant}$ ). Hygrothermally-aged thin-films prepared on Pt/PtO<sub>x</sub> exhibit an intensity  
 distribution, concentrated at  $q_p = 0$ , which indicates more domains are orientated parallel  
 to the surface. A domain orientation parameter,  $O.P.$ , quantifies the anisotropy of such  
 distributions:<sup>3</sup>

$$O.P. = \langle \cos^2 \chi \rangle = \frac{\int_0^{\pi/2} I(\chi) \sin(\chi) \cos^2 \chi d\chi}{\int_0^{\pi/2} I(\chi) \sin(\chi) d\chi} \langle S \rangle_{\text{domain}} = \frac{1}{2} \langle 3\omega_{\text{ori}} - 1 \rangle \quad [1]$$

where *O.P.* is between 0 (domains perpendicular to the substrate) and 1 (domains parallel to the substrate) and is 0.33 for an isotropic structure (random domain orientation). Fig. 1c shows the *O.P.* for PFSA thin-films increases upon hygrothermal ageing. In addition, there is a higher *O.P.* for aged long side-chain PFSA (Nafion over 3M), revealing the possible role of pendant chain chemistry in these governing interactions.<sup>18</sup> Fig. 1c shows increased nanostructural orientation on Pt/PtO<sub>x</sub> compared to Si/SiO<sub>x</sub>, in both as-cast (unaged) and aged state. Aged thin-films on Pt/PtO<sub>x</sub>, also showed greater *O.P.* distribution probably due to the dynamic interactions between water and Pt/ionomer interface.<sup>3,17,19,20</sup>



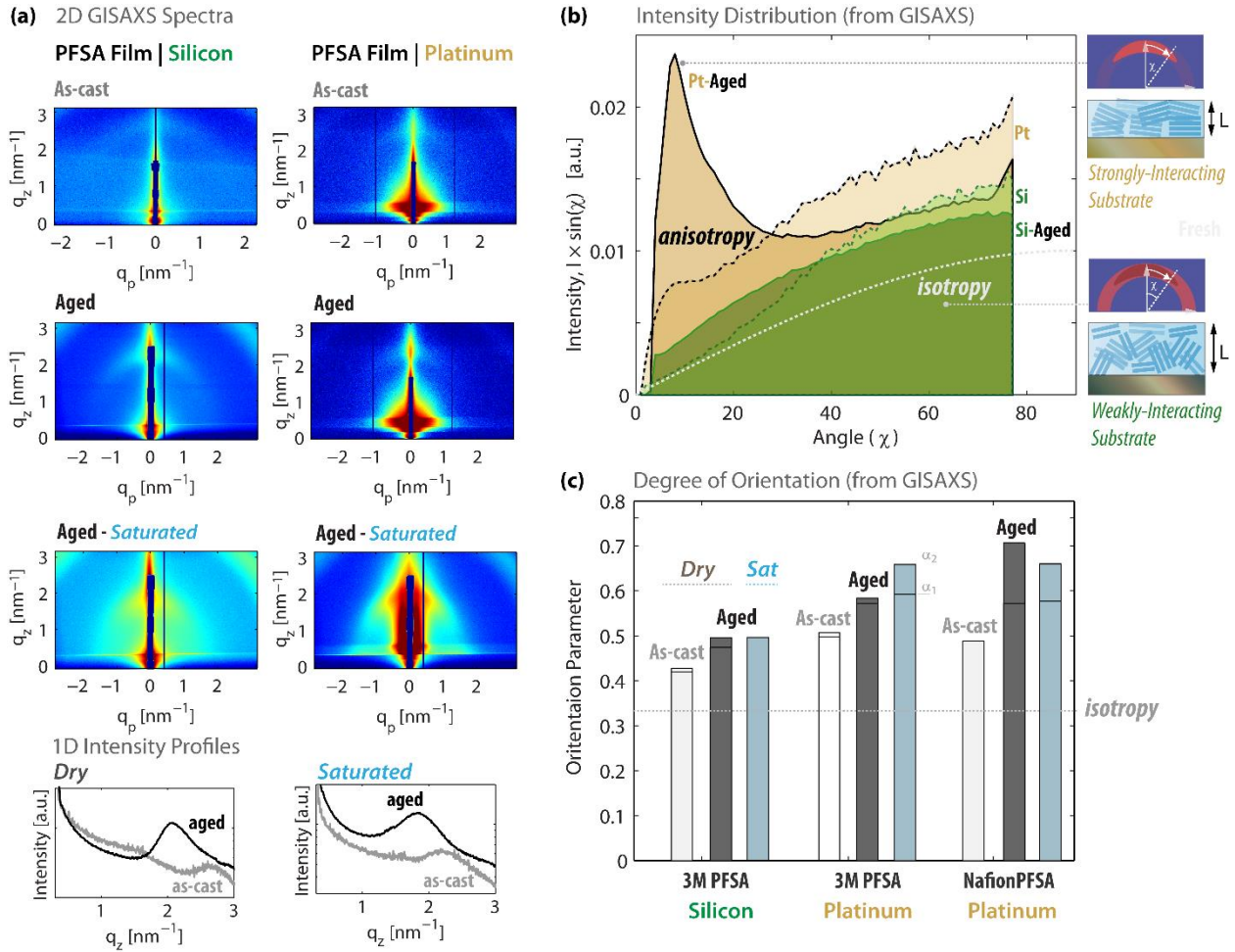
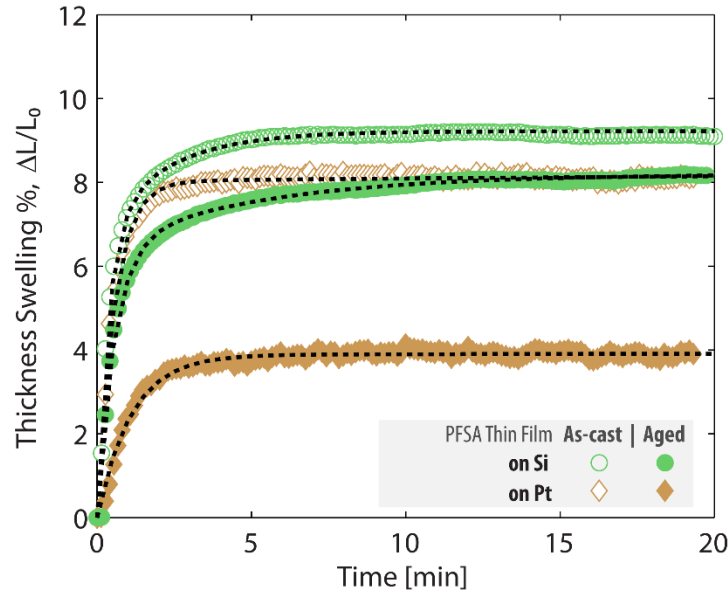


Figure 1: (a) 2D GISAXS images of as-cast (unaged) and hygrothermally aged PFSA (3M, 825g/mol equivalent weight) thin-films spin-cast on Si/SiO<sub>x</sub> and Pt/PtO<sub>x</sub> substrate in dry (33%) and saturated (100% RH) conditions at 26 °C. 1D intensity profiles are shown below for the 3M PFSA films on Si/SiO<sub>x</sub> substrate, based on the 2D images. (b) Intensity distribution as a function of azimuthal angle,  $\chi$ , for the ionomer peak. The solid and dashed lines represent the aged and as-cast samples, respectively, and the dotted line shows the distribution calculated for an ideal isotropic case. (c) Orientation parameter calculated from the distributions in (b). The low and high bars correspond to low and high incidence angle. (See SI for details).

The effect of hygrothermal ageing on ionomer swelling extent and kinetics was captured by *in-situ* spectroscopic ellipsometry. Fig. 2 compares swelling of aged and as-cast PFSA ionomer thin-films on Si/SiO<sub>x</sub> and Pt/PtO<sub>x</sub> substrates at 97% RH. In contrast to hygrothermally-aged films coated on Si/SiO<sub>x</sub>, which show a 12% reduction in swelling, aged films on Pt/PtO<sub>x</sub> exhibit a 50% reduction in extent of swelling normal to the substrate. For comparison, the same water-uptake reduction from reference (unaged) bulk PFSA

119 (~50  $\mu\text{m}$  thick) would require 100 days of hygrothermal ageing;<sup>21</sup> this difference between  
 120 bulk and thin-film aging highlights the enhanced interplay of confinement and substrate on  
 121 thin-film PFSA. The effect of ageing is amplified on strongly-interacting substrates like  
 122 Pt/PtO<sub>x</sub>,<sup>3,17,19,22</sup> which accelerates the ageing process.



123  
 124 Figure 2: Time-dependent fractional thickness swelling of PFSA (3M) thin-films (nominal  
 125 thickness,  $L_0 \approx 34$  nm) spin cast on Si/SiO<sub>x</sub> and Pt/PtO<sub>x</sub> substrates during humidification from 0 to  
 126 97 % RH. Data are shown for as-cast (unaged) and aged (at 85% RH, 70 °C for 4 days) films. The  
 127 dashed lines are best-fit to the measured data (symbols) using a two-term exponential expression,  
 128 discussed later.

129 To quantify this explicitly, ageing-induced changes in thin-film nanostructure (Fig.  
 130 1) can be correlated with water-sorption dynamics by investigating swelling kinetics (Fig.  
 131 2). The time-dependent swelling process is analyzed by fitting the normalized transient  
 132 thickness change (Fig. 2) to a two-term exponential expression<sup>1</sup>:

$$133 \quad \frac{L(t)-L_0}{L_\infty-L_0} = 1 - A \exp\left(-\frac{t}{\tau_1}\right) - (1-A) \exp\left(-\frac{t}{\tau_2}\right) \quad [2]$$

134 where  $\tau_1$  and  $\tau_2$  are time constants for the short-term (fast, diffusional transport) and long-  
 135 term (slow, physical relaxation and interfacial transport) swelling processes,

136 respectively.<sup>1,23</sup> Fig. 3a shows the inverse time constant of water sorption kinetics,  $k_s = 1/\tau$ ,  
137 against *O.P.* Assuming one-dimensional swelling in thin-films, interfacial transport and  
138 water diffusion can be estimated from characteristic time constants  $\tau_2 (=L/k_{int})$  and  $\tau_1$   
139  $(=L^2/D_{water})$ , respectively.  $D_{water}$  in ionomer thin-films explored here ranges from  $10^{-12}$  cm<sup>2</sup>/s  
140 to  $10^{-13}$  cm<sup>2</sup>/s; reduction in  $D_{water}$  tracks with increasing *O.P.* and is on the same order of  
141 magnitude as those reported by Eastman *et. al.*<sup>24</sup> Unaged films on Pt/PtO<sub>x</sub> possess strong  
142 orientation and ageing increases structural parallel orientation on both supports,  
143 presumably impacting through-plane water transport. Considering the primary governing  
144 water transport mechanism to be interfacial transport,  $k_{int} = L/\tau_2$  (ranging from  $10^{-6}$  to  $10^{-8}$   
145 cm/s) illustrates a different aspect of ageing. Change in *O.P.* is strongly coupled with  
146 diffusional transport, which is accompanied by swelling at early times, while interfacial  
147 relaxation becomes dominant at longer time-scales ( $\tau_1 > \tau_2$ ) and is dependent on *O.P.* to a  
148 lesser extent. For comparable ageing-induced change in *O.P.*, thin-films on Pt/PtO<sub>x</sub> show  
149 higher time constant relative to Si/SiO<sub>x</sub>, perhaps due to differences in substrate/ionomer  
150 interaction compounded by physical ageing (relaxation) that has been shown to be  
151 accelerated on metal supports.<sup>20,22,25</sup> However, the key takeaway is ageing-induced  
152 morphological rearrangement (*O.P.*) is inversely correlated to characteristic rate for  
153 swelling ( $k_s$ ) representing water transport kinetics (or time constant is proportional to *O.P.*,  
154 i.e.,  $\tau \propto 1/k_s \propto O.P.$ ).

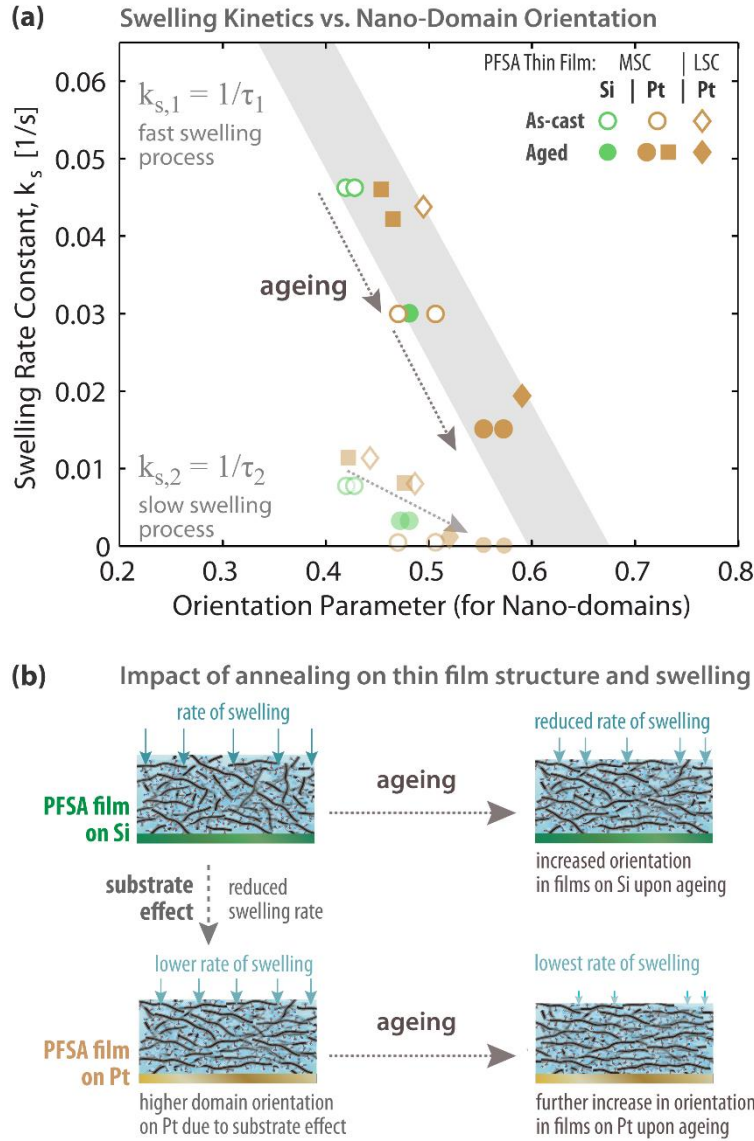


Figure 3: (a) Swelling rate constants of as-cast (unaged) and aged 3M (■,●) and Nafion (◆) PFSA thin-films during humidification to saturation (from ellipsometry) plotted against the orientation parameter of the same film in dry condition (from GISAXS). All the films were annealed after casting, except the unannealed 3M film on Pt (■), which is shown for comparison. Two rate constants are plotted for each case, representing the fast and slow swelling processes. (From Eq. (2)). (b) The schematics illustrate the inverse relationship between increasing domain orientation (parallel to the interfaces) and kinetics of swelling. The shaded region is shown as the guide for-the-eye.

Ionomer hydration controls transport properties like ion conduction and gas diffusion. Tunable nanostructures that control hydration and transport pathways can be designed via synthesis or processing techniques for well-ordered ionomers like sulfonated block or graft copolymers.<sup>2</sup> A similar attempt is made here via hygrothermal ageing of disordered thin-film PFSA, whose properties are subject to additional surface interaction effects that are heightened with finite size. Previous studies have demonstrated that alignment of hydrophilic moieties at the ionomer surface, governed by the interactions of the ionomer with vapor or liquid,<sup>3,26–28</sup> is related to mass-transport of water.<sup>1,26,28</sup> Findings in this work reflect similar stimulus(hygrothermal ageing)-driven, surface(Pt/PtO<sub>x</sub>)-controlled, and chemistry (side-chain) influenced preferential orientation resulting in water transport limitations in ionomer thin-films. A number of postulations are made here to explain this direct correlation and reduction in ionomer water transport/swelling rate with increase in *O.P.*:

(1) Increasing backbone alignment parallel to the substrate selectively lowers through-plane water transport by lowering hydrophilic surface area and increasing tortuosity, similar to the effect of structurally-induced orientation on ion transport.<sup>7,8</sup> Ageing-induced chain orientation increases the fraction of -SO<sub>3</sub><sup>-</sup> moieties near the substrate, intensifies their pairwise interactions, which could further enhance orientation, and reduces swelling and swelling kinetics perpendicular to the substrate.

(2) Coupled with previous postulate on kinetics, hygrothermal ageing induces order in the nanostructure, enabling the ionomer to access different quasi-equilibrium states.<sup>29</sup> This is in similar vein to processing induced alignments in di-block polymers.<sup>2,16,30</sup> Such a structure could preserve substrate/film interactions that

perpetuate and stabilize the chain configurations that could alter swelling governed by thermodynamic equilibrium. Comparative ageing and morphological studies in other solvents could elucidate the role of solvent and reversibility in achieving alternative structures to decouple the kinetic and thermodynamic effects.

(3) Distinct from the other two possible explanations is sulfonic anhydride formation, similar to that occurring in bulk PFSA.<sup>9,10,21</sup> Anhydride formation increases equivalent weight via physical crosslinking of ionomer chains and reduces water uptake. This explanation would imply that enhanced order and interaction on Pt/PtO<sub>x</sub> accelerates anhydride formation in ionomer over Si/SiO<sub>x</sub> support. Spectroscopic studies on aged thin-films could provide insight into presence of other forms of degradation and anhydride formation.

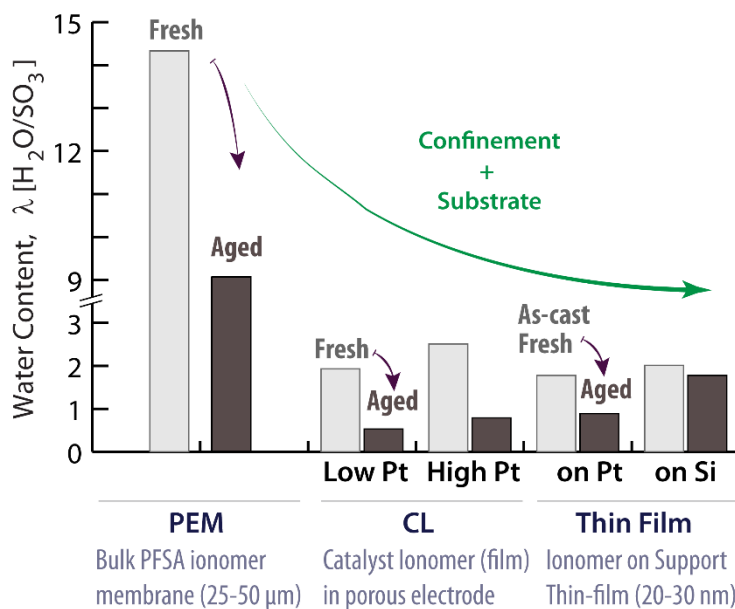


Figure 4: Comparison of maximum ionomer water content (at 95-97%RH) in bulk membrane,<sup>10</sup> catalyst layer (CL), and thin-films on a support (PFSA for PEM is Nafion, while for CL and thin-films 3M PFSA is used. See SI for full description of materials and treatment conditions).

These results on thin-film swelling are consistent with our hydration measurements on the unaged and aged catalyst layers (CLs) of varying Pt loading (see SI); higher Pt loading reflects significant reduction in water uptake with hygrothermal ageing compared to low-loaded CL (Fig. 4). Thus, findings herein shed light into the ionomer structure-related origins of the performance limitations in fuel-cell electrodes that may occur during operation, and how they might be influenced by the dynamic substrate-ionomer interactions. It must be noted that correlating ionomer's structure-swelling changes to performance is not trivial due to variations in the Pt/ionomer interface such as surface roughness (Figure S2 in Supporting Information) and substrate composition along with environmental effects (reducing or oxidizing), which were shown to consequently alter thin-film swelling.<sup>17</sup>

This letter reports compelling evidence for the existence of an explicit correlation between the orientation of nano-domains and swelling kinetics in PFSA ionomer thin-films, which is evidenced by ageing-induced changes in the film's nanostructure and swelling. The higher the orientation parallel to film surface, the slower the transport normal to surface. Stronger interactions between ionomer side-chains and Pt/PtO<sub>x</sub> enhances the impact of hygrothermal ageing by preferentially aligning more of the backbone parallel to the substrate. Domain alignment and re-alignment caused by environment (e.g., hygrothermal ageing and saturation) and ionomer/substrate interactions dictates swelling behavior and water transport in thin-films. Notably, the temperature used in this study for ageing is much less than the initial annealing temperatures (70 °C vs. 140-160 °C), which underscores the role of water as an important stressor driving the film towards structural reorganization that influence material properties. Results presented herein provide new

229 insights into the impact of environmental conditioning on inducing morphological changes  
230 in ionomer thin-films, a phenomenon of great importance for elucidating and controlling  
231 their structure/function relationship and transport response at dynamic interfaces in energy  
232 conversion devices.

233



## 234    **Acknowledgements**

235    Authors would like to thank William Tong, Peter Dudenas, Julie Fornaciari, and Andrew  
236    Crothers for helpful discussions, insights and supplemental work. We thank Rodney Borup  
237    of LANL for discussions on ageing procedures and help with CL preparations, and Steve  
238    Hamrock and Mike Yandrasits from 3M for providing ionomer dispersions. AK  
239    acknowledges support from the Fuel Cell Technologies Office, Energy Efficiency and  
240    Renewable Energy Office, of the U.S. Department of Energy (DOE), under contract no.  
241    DE-AC02-05CH11231. Funding support for MT was provided by University of California  
242    Chancellors Fellowship. We thank Chenhui Zhu, Polite Stewart and Eric Schaible for their  
243    assistance with facilitating the equipment at the Advanced Light Source (ALS) beamline  
244    7.3.3, supported by the Office of Science, Office of Basic Energy Sciences, of the U.S.  
245    DOE (Contract No. DE-AC02-05CH11231). This work made use of facilities at the Joint  
246    Center for Artificial Photosynthesis supported through the Office of Science of the U.S.  
247    DOE under Award Number DE-SC0004993<sup>†</sup>.

248

249    **Supporting Information:**

250    Associated Content: Full experimental methods are provided in detail in Supporting Information.

251

252   **Reference**

- 253   (1)   Kusoglu, A.; Weber, A. Z. New Insights into Perfluorinated Sulfonic-Acid Ionomers.  
254       *Chem. Rev.* **2017**, *117*, 987–1104.
- 255   (2)   Park, M. J.; Hong, J.; Kim, S. Y. Role of Nanostructures in Polymer Electrolytes for  
256       Energy Storage and Delivery. In *ACS Symposium Series 1096; Polymers for Energy*  
257       *Storage and Delivery: Polyelectrolytes for Batteries and Fuel Cells*; 2012; pp 129–146.
- 258   (3)   Kusoglu, A. Ionomer Thin Films in PEM Fuel Cells. In *Encyclopedia of Sustainability*  
259       *Science and Technology*; Meyers, R., Ed.; Springer, New York, NY, 2018.
- 260   (4)   Kongkanand, A.; Gu, W.; Mathias, M. F. Proton-Exchange Membrane Fuel Cells with  
261       Low-Pt Content. In *Encyclopedia of Sustainability Science and Technology*; 2018.
- 262   (5)   Tesfaye, M.; Kushner, D. I.; McCloskey, B. D.; Weber, A. Z.; Kusoglu, A. Thermal  
263       Transitions in Perfluorosulfonated Ionomer Thin-Films. *ACS Macro Lett.* **2018**, 1237–  
264       1242.
- 265   (6)   DeCaluwe, S. C.; Baker, A. M.; Bhargava, P.; Fischer, J. E.; Dura, J. A. Structure-  
266       Property Relationships at Nafion Thin-Film Interfaces: Thickness Effects on Hydration  
267       and Anisotropic Ion Transport. *Nano Energy* **2018**, *46*, 91–100.
- 268   (7)   Ono, Y.; Nagao, Y. Interfacial Structure and Proton Conductivity of Nafion at the Pt-  
269       Deposited Surface. *Langmuir* **2016**, *32*, 352–358.
- 270   (8)   Nagao, Y. Proton-Conductivity Enhancement in Polymer Thin Films. *Langmuir* **2017**, *33*,  
271       12547–12558.
- 272   (9)   Naudy, S.; Collette, F.; Thominet, F.; Gebel, G.; Espuche, E. Influence of Hygrothermal

- 273 Aging on the Gas and Water Transport Properties of Nafions Membranes. *J. Memb. Sci.*  
274 **2014**, *451*, 293–304.
- 275 (10) Shi, S.; Dursch, T. J.; Blake, C.; Mukundan, R.; Borup, R. L.; Weber, A. Z.; Kusoglu, A.  
276 Impact of Hygrothermal Aging on Structure/Function Relationship of Perfluorosulfonic-  
277 Acid Membrane. *J. Polym. Sci. Part B Polym. Phys.* **2016**, *54*, 570–581.
- 278 (11) Shi, S.; Chen, G.; Wang, Z.; Chen, X. Mechanical Properties of Nafion 212 Proton  
279 Exchange Membrane Subjected to Hygrothermal Aging. *J. Power Sources* **2013**, *238*,  
280 318–323.
- 281 (12) Onishi, L. M.; Prausnitz, J. M.; Newman, J. Water - Nafion Equilibria. Absence of  
282 Schroeder's Paradox. **2007**, 10166–10173.
- 283 (13) Hensley, J. E.; Way, J. D.; Dec, S. F.; Abney, K. D. The Effects of Thermal Annealing on  
284 Commercial Nafion Membranes. *J. Memb. Sci.* **2007**, *298*, 190–201.
- 285 (14) Stewart-Sloan, C. R.; Olsen, B. D. Protonation-Induced Microphase Separation in Thin  
286 Films of a Polyelectrolyte-Hydrophilic Diblock Copolymer. *ACS Macro Lett.* **2014**, *3*,  
287 410–414.
- 288 (15) Gu, X.; Gunkel, I.; Hexemer, A.; Russell, T. P. Controlling Domain Spacing and Grain  
289 Size in Cylindrical Block Copolymer Thin Films by Means of Thermal and Solvent Vapor  
290 Annealing. *Macromolecules* **2016**, *49*, 3373–3381.
- 291 (16) Sinturel, C.; Vayer, M.; Morris, M.; Hillmyer, M. A. Solvent Vapor Annealing of Block  
292 Polymer Thin Films. *Macromolecules* **2013**, *46*, 5399–5415.
- 293 (17) Tesfaye, M.; MacDonald, A. N.; Dudenas, P. J.; Kusoglu, A.; Weber, A. Z. Exploring

294 Substrate/Ionomer Interaction under Oxidizing and Reducing Environments. *Electrochem.*  
295 *commun.* **2018**, 87, 86–90.

296 (18) Kusoglu, A.; Dursch, T. J.; Weber, A. Z. Nanostructure/Swelling Relationships of Bulk  
297 and Thin-Film PFSA Ionomers. *Adv. Funct. Mater.* **2016**, 26, 4961–4975.

298 (19) Yagi, I.; Inokuma, K.; Kimijima, K.; Notsu, H. Molecular Structure of Buried  
299 Perfluorosulfonated Ionomer/Pt Interface Probed by Vibrational Sum Frequency  
300 Generation Spectroscopy. *J. Phys. Chem. C* **2014**, 118, 26182–26190.

301 (20) Kodama, K.; Motobayashi, K.; Shinohara, A.; Hasegawa, N.; Kudo, K.; Jinnouchi, R.;  
302 Osawa, M.; Morimoto, Y. Effect of the Side-Chain Structure of Perfluoro-Sulfonic Acid  
303 Ionomers on the Oxygen Reduction Reaction on the Surface of Pt. *ACS Catal.* **2018**, 8,  
304 694–700.

305 (21) Collette, F. M.; Lorentz, C.; Gebel, G.; Thominette, F. Hygrothermal Aging of Nafion. *J.*  
306 *Memb. Sci.* **2009**, 330, 21–29.

307 (22) Selvan, M. E.; He, Q.; Calvo-Munoz, E. M.; Keffer, D. J. Molecular Dynamic Simulations  
308 of the Effect on the Hydration of Nafion in the Presence of a Platinum Nanoparticle. *J.*  
309 *Phys. Chem. C* **2012**, 116, 12890–12899.

310 (23) Kongkanand, A. Interfacial Water Transport Measurements in Nafion Thin Films Using a  
311 Quartz-Crystal Microbalance. *J. Phys. Chem. C* **2011**, 115, 11318–11325.

312 (24) Eastman, S. A.; Kim, S.; Page, K. A.; Rowe, B. W.; Kang, S.; Soles, C. L.; Yager, K. G.  
313 Effect of Confinement on Structure, Water Solubility, and Water Transport in Nafion Thin  
314 Films. *Macromolecules* **2012**, 45, 7920–7930.

- 315 (25) Kushner, D. I.; Hickner, M. A. Substrate-Dependent Physical Aging of Confined Nafion  
316 Thin Films. *ACS Macro Lett.* **2018**, 7, 223–227.
- 317 (26) Novitski, D.; Holdcroft, S. Determination of O<sub>2</sub> Mass Transport at the Pt | PFSA Ionomer  
318 Interface under Reduced Relative Humidity. *ACS Appl. Mater. Interfaces* **2015**, 7, 27314–  
319 27323.
- 320 (27) Hwang, G. S.; Parkinson, D. Y.; Kusoglu, A.; Macdowell, A. A.; Weber, A. Z.  
321 Understanding Water Uptake and Transport in Nafion Using X-ray Microtomography.  
322 *ACS Macro Lett.* **2013**, 2, 288–291.
- 323 (28) He, Q.; Kusoglu, A.; Lucas, I. T.; Clark, K.; Weber, A. Z.; Kostecki, R. Correlating  
324 Humidity-Dependent Ionically Conductive Surface Area with Transport Phenomena in  
325 Proton-Exchange Membranes. *J. Phys. Chem. B* **2011**, 115, 11650–11657.
- 326 (29) Kim, T. H.; Yi, J. Y.; Jung, C. Y.; Jeong, E.; Yi, S. C. Solvent Effect on the Nafion  
327 Agglomerate Morphology in the Catalyst Layer of the Proton Exchange Membrane Fuel  
328 Cells. *Int. J. Hydrogen Energy* **2017**, 42, 478–485.
- 329 (30) Kim, J.; Kim, B.; Jung, B.; Kang, Y. S.; Ha, H. Y.; Oh, I. H.; Ihn, K. J. Effect of Casting  
330 Solvent on Morphology and Physical Properties of Partially Sulfonated Polystyrene-  
331 Block-Poly(Ethylene-Ran-Butylene)-Block-Polystyrene Copolymers. *Macromol. Rapid*  
332 *Commun.* **2002**, 23, 753–756.